Single-Molecule Magnets

Coupling Dy₃ Triangles to Maximize the Toroidal Moment**

Shuang-Yan Lin, Wolfgang Wernsdorfer, Liviu Ungur, Annie K. Powell, Yun-Nan Guo, Jinkui Tang,* Lang Zhao, Liviu F. Chibotaru,* and Hong-Jie Zhang*

Compounds constructed by utilizing a toroidal arrangement of dipoles are attractive for applications in multiferroic materials.[1] A toroidal arrangement of dipole moments can be envisaged, for example, by a current flowing through a solenoid bent into a torus or else by a similarly organized arrangement of magnetic dipoles.[2] This is proposed as the primary order parameter for a multiferroic material.[1a,3] Recent efforts at the boundary where the description of solid-state systems meets that of molecular-based materials has revealed some interesting shifts in accepted paradigms. For example, concepts such as magnetism, magnetocaloric effects, and ferroelectrics can be viewed as properties recognizable at the condensed as well as molecular level, and there is growing interest in exploring the boundaries between these two worlds.[4] Particularly relevant to these endeavors is the consideration of bounded (confined) metal oxide structures having toroidal moments compared with their solid-state infinite analogues.[2b,5] On the other hand, it can also be difficult to separate purely molecular-based effects from those resulting from a resultant toroidal moment arising through a long-range interaction.[6]

The recently investigated Dy₃ triangle (prototype Dy₃)[7] is one of the four possible ingredients for creating multiferroic systems that should manifest two or more out of ferroelectric, ferromagnetic, ferroelastic, and ferrotoroidal behavior.[1c,8]

Subsequently, a Dy₄ single-molecule magnet (SMM),[9] a **Dy₆-1** SMM,[10] and a heterometallic CuII/DyIII₃ 1D polymer (Dy₃Cu)[4c] have been reported to show a toroidal magnetic moment in the ground state. The coupled **Dy₆-1** SMM that results from coupling two of the original Dy₃ triangles shows enhanced relaxation dynamics compared with the precursor Dy₃,[7] but the overall anisotropy and spin structure lead to a reduced toroidal magnetization.[10] Dy₃Cu is constructed by combining alternating trinuclear Dy₃ SMM-building blocks and enantiopure, chiral copper(II) complexes.[4c] The discrete Dy₃ triangular molecule, which can be regarded as an archetypical toroidal manifestation of an antiferromagnetic arrangement of Ising spins, has been reported and extensively investigated by us.[7,11] This system not only shows an essentially nonmagnetic spin ground state but also possesses a toroidal moment as described above and SMM behavior deriving from its excited states. These factors offer perspectives for the fundamental understanding and applications of quantum computation and data storage in molecular nano-magnets.[6,12] The toroidal ground spin state structure analysis of the Dy₃Cu system reveals that the combination of molecular chirality and the toroidal magnetism are predicted to provide multiferroic behavior only under applied fields.[4c] Thus the synthesis of compounds with utilizable large toroidal magnetic moments is a significant challenge.

Given these promising results, our aim was to pursue the use of the toroidal Dy₃ building block further to enhance the molecular toroidal magnetization and with the view to furthering application in multiferroics. We thus decided to focus our attention on the rearrangement of Dy₃ triangles in addition to keeping in mind a systematic survey of the structural types and characteristics of compounds showing toroidal magnetic moments. Herein we report the successful combination of two Dy₃ triangles in an edge-to-edge arrangement. The resulting compound shows SMM behavior with enhancement of the toroidal magnetization. In comparison to all other combinations of the Dy₃ triangle that have been reported, this system is the best construction to preserve perfectly and enhance greatly the toroidal magnetization.

The reaction of H₃L, formed by the in situ condensation of 2,6-diformyl-4-methylphenol and ethanolamine, with Dy-(NO₃)₃·6H₂O in the presence of triethylamine under solvo-thermal condition, produces pale-yellow crystals of [Dy₆L₄-(μ₄-O)(NO₃)₄(CH₃OH)]·CH₃OH (**1**). As shown in Figure 1, the hexanuclear Dy₆ core can be regarded as the linkage of two [Dy₃(μ₃-O)₂(μ₂-O)₂] triangular units placed in an edge-to-edge arrangement by one μ₄-O²⁻ ion and four deprotonated phenol oxygen atoms from four ligands. The dihedral angle between the two Dy₃ planes in **1** is 29.656°, in contrast to the co-parallel planes in reported **Dy₆-1**. Each triangular unit is

[*] S. Y. Lin, Y. N. Guo, Prof. Dr. J. Tang, Dr. L. Zhao, Prof. H. J. Zhang
State Key Laboratory of Rare Earth Resource Utilization
Changchun Institute of Applied Chemistry, Chinese Academy of Sciences
Changchun 130022 (P. R. China)
E-mail: tang@ciac.jl.cn
hongjie@ciac.jl.cn

S. Y. Lin
University of Chinese Academy of Sciences
Beijing 100039 (P. R. China)

Prof. A. K. Powell
Institute of Inorganic Chemistry, Karlsruhe Institute of Technology
Engesserstrasse 15, 76131 Karlsruhe (Germany)

Dr. W. Wernsdorfer
Institut Néel, CNRS & Université J. Fourier, BP 166
25 Avenue des Martyrs, 38042 Grenoble (France)

Dr. L. Ungur, Prof. L. F. Chibotaru
Division of Quantum and Physical Chemistry, Department of Chemistry, Katholieke Universiteit Leuven
Celestijnenlaan 200F, 3001 Leuven (Belgium)
E-mail: liviu.Chibotaru@chem.kuleuven.be
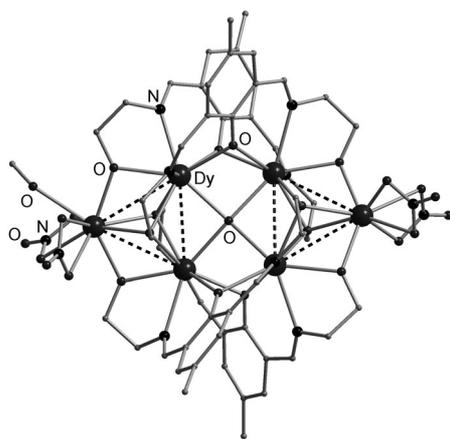
Figure 1. The molecular structure of [Dy$_6$L$_4$(μ_4-O)(NO$_3$)$_4$-(CH$_3$OH)]·CH$_3$OH (**1**). Solvent molecules and hydrogen atoms are omitted for clarity.

Figure 2. Field dependence of the molar magnetization at 1.9 K. The solid line corresponds to the best fit. Inset: temperature dependence of the magnetic susceptibility at different fields.

capped by two μ_3-O alcohol oxygen atoms from one arm of ligands above or below, that is by ethoxy rather than by the μ_3-OH caps of the original triangle.[7,10,13] The μ_2-O alcohol oxygen atoms from the other arms of the same ligands bridge edges of the triangles. The coordination spheres of the dysprosium ions are completed by a methanol molecule and four nitrate ions, generating eight-coordinate Dy1/Dy2/Dy3/Dy4/Dy5 centers with distorted square antiprismatic geometries and a nine-coordinate Dy6 ion with a distorted monocapped square antiprismatic geometry (Supporting Information, Figure S1). The triangular Dy$_3$ units in **1** are less equilateral than the prototype Dy$_3$ with Dy···Dy distances in range 3.3934(3)–3.5412(4) Å.

It is noteworthy that the μ_4-O^{2-} ion links two Dy$_3$ triangles in the center and four deprotonated phenol oxygen atoms further consolidate the Dy$_6$ construction in the periphery to arrange the two Dy$_3$ triangles in a robust edge-to-edge arrangement. Such a stable Dy$_3$ + Dy$_3$ construction will enhance the toroidal magnetic moment of the molecule (see below).

The packing arrangement of **1** reveals that right-hand (Δ) and left-hand (Λ) configuration helicates are in alternate layers along the crystallographic *a*, *b*, and *c* axes (Supporting Information, Figures S2 and S3).

The static magnetic behavior of **1** closely resembles that of the prototype Dy$_3$ (Figure 2; Supporting Information, Figure S4). As shown in Figure S4, the $\chi_M T$ value (measured under 1 kOe dc field) at 300 K of 85.5 cm^{3}Kmol^{-1} is close to the expected value for six uncoupled Dy^{III} ions (^{6}H$_{15/2}$, $L = 5$, $g = 4/3$) and gradually decreases upon lowering the temperature to 20 K, then decreasing abruptly to 10.3 cm^{3}K mol^{-1} at 2.0 K. In the low-temperature susceptibility, a maximum is observed around $T = 7$ K under 1 kOe dc field, in contrast with 3 K in **Dy$_6$-1**. However, the susceptibility shows a constant increase with an applied field of 13 kOe (Figure 2). This constant increase suggests the presence of weak antiferromagnetic (AF) interactions, which are overcome by the application of a moderate field. The magnetization (*M*) measured under variable field at 1.9 K shows an obvious inflection around 9 kOe, and reaches a maximum value
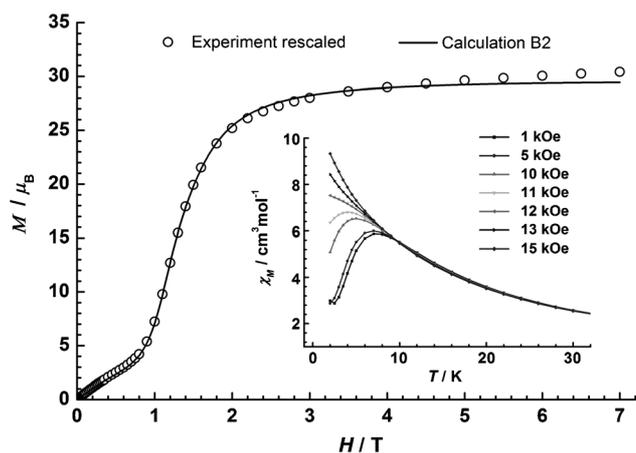
32.9 μ_B at about 70 kOe. Interestingly, the unusual well-defined step observed in **1** was seen for the prototype Dy$_3$ and the Dy$_3$Cu system but not in the other arrangements of Dy$_3$ triangles, where this step is absent[13a] or less pronounced.[10] The lack of saturation of the *M* versus *H* data at 70 kOe can be attributed to crystal-field effects and the presence of weak antiferromagnetic interactions that make the low-lying excited states accessible, while the non-superposition of the *M* versus *H/T* data (Supporting Information, Figure S5) implies the presence of significant magnetic anisotropy.[7,14] All aspects of the static magnetic behavior reveal that the ground state of **1** is a non-magnetic doublet as the case of prototype Dy$_3$, as supported by the ab initio calculations (see below).

Single crystals of **1** were studied further using the micro-SQUID technique. A stepped shape of the magnetization hysteresis (Figure 3; Supporting Information, Figure S6) is observed with a steep rise at the crossing field $H_c = \pm 0.95$ T, which is found to be in good agreement with measurements on polycrystalline samples. As the following ab initio calculations show, the steep rise is due to the Zeeman crossing of the ground level with the lowest Zeeman component of the second excited state situated at 7.7 cm^{-1} and having three times larger magnetic moment compared to the ground state (see below). The difference in the present compound from the
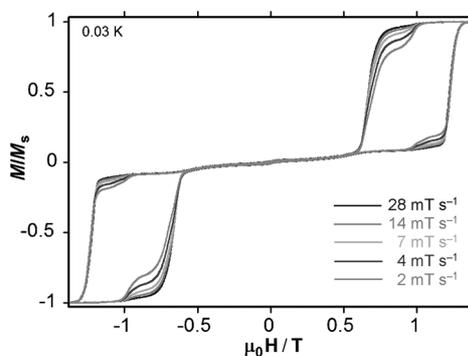

Figure 3. Hysteresis loops for **1** at different field sweep rates at 0.03 K.

prototype Dy$_3$[11b,15] is the presence of a large magnetic moment in the ground state, which results in a larger crossing field than in the previous compound. The reason for that is in the orientations of local anisotropy axes, which differ much more from an equilateral triangle in the present compound than in the prototype Dy$_3$. In turn, this difference is dictated by the geometry of the two compounds, which is close to an equilateral triangle in the case of prototype Dy$_3$ while it is of much lower symmetry for the present Dy$_6$. Furthermore, the observed larger hysteresis indicates that the "quantum mixing" in **1** is smaller than that in the prototype Dy$_3$ because the quantum mixing increases the tunneling at the energy level crossings, and the larger the quantum mixing, the smaller the hysteresis.[16]

Given the unusual slow relaxation behavior in prototype Dy$_3$, the alternating current (ac) susceptibilities were investigated from the ac susceptibility measurements (Figure 4; Supporting Information, Figures S7–S12). Under a zero dc field, the variable-temperature ac susceptibilities show the temperature dependence maximum, signaling the freezing of the spins by the anisotropy barriers, which is typical for SMM behavior. Unlike most Ln-SMMs, the drop in the out-of-phase and in-phase susceptibility on cooling at low temperatures most likely originates from an antiferromagnetic interaction between the Dy ions, which tends to create a nonmagnetic ground state.[7,17] The broad shoulders between 4 and 15 K at 10–1000 Hz suggest the coalescence of the two peaks, signal-
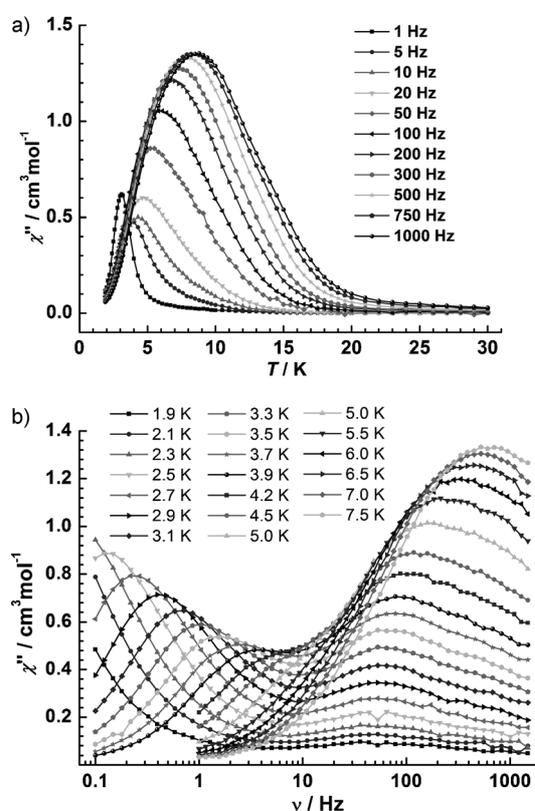

Figure 4. a) Temperature- and b) frequency-dependent out-of-phase ac susceptibility for **1** under a zero dc field. The solid lines are to guide the eye.

ing the possibility that two relaxation processes are equally prominent. Indeed, variable-frequency ac susceptibility measurements clearly show the occurrence of two distinct peaks in χ''. The intensity of the high frequency peak increases with temperature at the expense of the low frequency peak. The relaxation times were thus extracted from the frequency dependent data and plotted as a function of $1/T$. The effective energy barriers based on the Arrhenius law ($\tau = \tau_0 \exp(U_{eff}/kT)$) are 33.9 and 40.7 K with pre-exponential factors (τ_0) of 5.8×10^{-8} and 1.2×10^{-7} s for the high frequency relaxation and low frequency relaxation, respectively (Supporting Information, Figure S8). The multiple relaxation processes are also evident from the Cole–Cole plots that cannot be well fitted by the sum of two modified Debye functions (Supporting Information, Figures S9, S10, and Table S1).[18] The observation of multiple relaxation processes is the result of the presence of distinct anisotropic centers and the exchange interactions.[19]

To gain further insight into the nature of the local anisotropy of the dysprosium sites and the lowest exchange states, ab initio calculations[20] on the individual Dy^{III} magnetic sites in **1** were performed (Supporting Information, Table S2). The results (Table 1; Supporting Information,

Table 1: Energies of the low-lying Kramers doublets [cm^{-1}] and main values of g tensors for the lowest Kramers doublet with basis set 2.

	Dy1	Dy2	Dy3	Dy4	Dy5	Dy6
	0.000	0.000	0.000	0.000	0.000	0.000
	172.293	160.888	141.581	167.058	249.721	191.646
	223.498	221.348	201.659	201.442	390.563	349.618
	261.612	258.477	238.687	226.973	438.007	456.665
	304.214	299.988	279.964	266.020	474.709	492.971
	356.552	333.541	330.253	294.100	515.550	538.094
	472.533	422.458	465.156	376.734	540.067	590.162
	502.696	492.495	503.597	482.803	656.566	655.723
	3620.826	3626.571	3604.523	3629.168	3670.604	3630.742
g_X	0.0078	0.0054	0.0074	0.0106	0.0047	0.0067
g_Y	0.0152	0.0087	0.0127	0.0171	0.0069	0.0073
g_Z	19.734	19.656	19.739	19.687	19.783	19.821

Tables S3–S6) show the ground Kramers doublet on each dysprosium site is well separated from the first excited state, whilst the g tensors are strongly axial. As expected, the corresponding directions of anisotropy axes in both triangles (Figure 5; Supporting Information, Tables S7–S9) are nearly tangential directions and lie almost in the plane of the corresponding Dy$_3$ triangles; that is, the local magnetic moments are arranged in a perfect toroidal fashion in both Dy$_3$ triangles, as the case in prototype Dy$_3$ system.

Given the strong axiality of Dy sites, the magnetic interactions between dysprosium sites, including contributions from magnetic dipole–dipole and exchange interactions, were simulated within the Ising exchange Hamiltonian,[4c,11a,c,21] and the calculation of exchange spectrum is done within the Lines model (see the Supporting Information).[11a] The values of the best Lines and Ising exchange parameters, obtained from the fitting of $\chi_M T(T)$ and $M(H)$ for **1** are listed in Table 2 and the Supporting Information, Table S10. Figure 2 and the Supporting Information, Figure S4 show
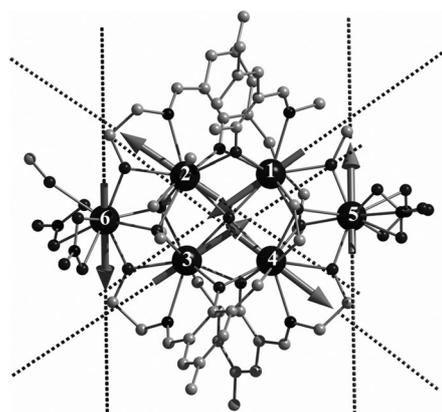
Figure 5. Main anisotropy axes (dashed lines) on Dy ions and local magnetizations (arrows) in the ground state in **1**.

Table 2: Ising magnetic interactions within and between the two triangles for **1**.

Interacting pair	J_{dip}	J_{exch}	$J_{total}=J_{dip}+J_{exch}$
1–2	7.03823	−2.08895	4.94927
1–3	−3.22677	5.97520	2.74843
1–4	5.44950	1.72148	7.17098
1–5	4.77403	3.14664	7.92066
2–3	5.34430	2.26746	7.61176
2–4	−3.29008	5.98198	2.69190
2–6	4.66512	3.10026	7.76539
3–4	7.03220	−1.89949	5.13271
3–6	4.61637	3.22955	7.84592
4–5	4.54610	3.56759	8.11369

the comparison of measured and calculated magnetic susceptibility and molar magnetization. It obvious that the sign and magnitude of the magnetic interactions inside each of the triangles (that is, interactions 1–4, 1–5, 4–5 and 2–3, 2–6, 3–6) are similar in strength and are the strongest interactions in this molecule. Moreover, these magnetic interactions are of similar strength as in prototype Dy₃ triangle. It is noteworthy that the magnetic interactions between triangles (that is, interactions 1–2 and 3–4) are relative stronger compared with those in **Dy₆-1**, which stabilize similar arrangement of toroidal moments in the ground states (Figure 5); that is, making the toroidal moment of the complex maximal possible.

The calculated energies (Supporting Information, Table S11 and Figure S13) show a magnetic state at 7.6 cm⁻¹ above the ground state compared with 0.4 cm⁻¹ in **Dy₆-1**. Therefore, it is not surprising to observe the appearance of a pronounced step in the *M* versus *H* curve. In contrast to the weak magnetic state in **Dy₆-1**, the first excited state in **1** stabilizes anticlockwise arrangement of the magnetic moments in both triangles.

Based on the ab initio calculations, a rationalization of the observed magnetic behavior can be explained reasonably by a toroidal magnetic state in **1**. Such a toroidal magnetic state has been inferred recently for **Dy₆-1** and the polymer Dy₃Cu. The **Dy₆-1** SMM has a weaker magnetic state compared with that in prototype Dy₃, which contributes to a less pronounced

toroidal moment; furthermore, interaction between the two triangles is too weak to stabilize the arrangement of the magnetic moments in each triangle. In the polymer Dy₃Cu, the involvement of different types of Dy ion in the exchange pathway led to the opposite arrangement of toroidal moments in the neighboring triangles, resulting in zero toroidal magnetization in the ground state. The toroidal magnetization is predicted to be only apparent in Dy₃Cu on application of an external magnetic field. In contrast, **1** shows obvious phenomena about toroidal moment and strong interactions between triangles. To further understand the nature of the toroidal magnetic moment and the lowest exchange states, comparisons between prototype Dy₃, Dy₃Cu, **Dy₆-1**, and **1** are listed in the Supporting Information, Table S12. From these data, it is evident that the obtained values for **1**, including the lowest calculated Kramers doublets, main values of the *g* tensors, Ising exchange parameters within a triangle, and the lowest magnetic excitation energies, are closest to those of the prototype Dy₃. We can therefore conclude that for both triangles of the edge-to-edge Dy₃ + Dy₃ arrangement, the spin chirality of the prototype Dy₃ triangle has been perfectly preserved. Most importantly, similar anticlockwise arrangements of toroidal moments in **1** are stabilized by strong couplings through the μ_4-O^{2-} ion between two triangles, in contrast to the weak interaction seen in **Dy₆-1**. Therefore, **1** is characterized by stronger magnetic chirality compared with the prototype Dy₃ (that is, by very large toroidal magnetic moment per unit cell), which may led to new possibilities in multiferroic systems and magnetic data storage technology.[1c]

In conclusion, modifying the prototype Dy₃ by employing a polydentate Schiff-base ligand, in effect, made it possible to arrange the Dy₃ triangles in an edge-to-edge arrangement whilst perfectly retaining the nonmagnetic ground state and SMM behavior. It is a very exciting finding that very large toriodal moments, which are useful for instance in molecule-based multiferroics, have been achieved thanks to strong couplings via a μ_4-O^{2-} ion, thereby stablizing two similar anticlockwise toroidal moments. Such a compound furthers the prospects for noncollinear magnetic molecules, potentially bringing the goals of molecule-based information storage, quantum computing, and induced ferrotoroidicity closer to reality. The present results provide a promising strategy for enhancing the toroidal magnetisms of polynuclear lanthanide-based compounds by fine-tuning the arrangements of the lanthanide ions and strengthening couplings between lanthanide ions.

Experimental Section

Synthesis of 1: Dy(NO₃)₃·6H₂O (0.30 mmol) reacted with the Schiff base (H₃L) formed by the in situ condensation of 2,6-diformyl-4-methylphenol (DFMP; 0.15 mmol) and ethanolamine (0.3 mmol) in 10 mL methanol in presence of Et₃N (0.45 mmol). The resulting reaction mixture was sealed in a reactor, heated to 90°C for 3 days, and then cooled slowly to room temperature to yield yellow single crystals suitable for X-ray diffraction. Yield: 21 mg, (18%, based on the metal). Elemental analysis (%) calcd for $C_{54}H_{68}Dy_6N_{12}O_{27}$: C 28.30, H 2.99, N 7.33; found C 27.90, H 2.96, N 7.11. IR (KBr):

[1] a) B. B. Van Aken, J.-P. Rivera, H. Schmid, M. Fiebig, *Nature* **2007**, *449*, 702–705; b) K. M. Rabe, *Nature* **2007**, *449*, 674–675; c) T. Kaelberer, V. A. Fedotov, N. Papasimakis, D. P. Tsai, N. I. Zheludev, *Science* **2010**, *330*, 1510–1512.

[2] a) V. M. Dubovik, V. V. Tugushev, *Phys. Rep.* **1990**, *187*, 145–202; b) C. Ederer, *Eur. Phys. J. B* **2009**, *71*, 349–354.

[3] N. A. Spaldin, M. Fiebig, M. Mostovoy, *J. Phys. Condens. Matter* **2008**, *20*, 434203.

[4] a) E. Coronado, D. Gatteschi, *J. Mater. Chem.* **2006**, *16*, 2513–2515; b) A. Dei, D. Gatteschi, *Angew. Chem.* **2011**, *123*, 12054–12060; *Angew. Chem. Int. Ed.* **2011**, *50*, 11852–11858; c) G. Novitchi, G. Pilet, L. Ungur, V. V. Moshchalkov, W. Wernsdorfer, L. F. Chibotaru, D. Luneau, A. K. Powell, *Chem. Sci.* **2012**, *3*, 1169–1176.

[5] a) C. Ederer, N. A. Spaldin, *Phys. Rev. B* **2007**, *76*, 214404; b) B. Mettout, P. Tolédano, M. Fiebig, *Phys. Rev. B* **2010**, *81*, 214417; c) P. Toledano, D. D. Khalyavin, L. C. Chapon, *Phys. Rev. B* **2011**, *84*, 094421; d) S. Valencia, A. Crassous, L. Bocher, V. Garcia, X. Moya, R. O. Cherifi, C. Deranlot, K. Bouzehouane, S. Fusil, A. Zobelli, A. Gloter, N. D. Mathur, A. Gaupp, R. Abrudan, F. Radu, A. Barthélémy, M. Bibes, *Nat. Mater.* **2011**, *10*, 753–758.

[6] D. I. Plokhov, A. I. Popov, A. K. Zvezdin, *Phys. Rev. B* **2011**, *84*, 224436.

[7] J. Tang, I. Hewitt, N. T. Madhu, G. Chastanet, W. Wernsdorfer, C. E. Anson, C. Benelli, R. Sessoli, A. K. Powell, *Angew. Chem.* **2006**, *118*, 1761–1765; *Angew. Chem. Int. Ed.* **2006**, *45*, 1729–1733.

[8] H. Schmid, *J. Phys. Condens. Matter* **2008**, *20*, 434201.

[9] P.-H. Guo, J.-L. Liu, Z.-M. Zhang, L. Ungur, L. F. Chibotaru, J.-D. Leng, F.-S. Guo, M.-L. Tong, *Inorg. Chem.* **2012**, *51*, 1233–1235.

[10] I. J. Hewitt, J. Tang, N. T. Madhu, C. E. Anson, Y. Lan, J. Luzon, M. Etienne, R. Sessoli, A. K. Powell, *Angew. Chem.* **2010**, *122*, 6496–6500; *Angew. Chem. Int. Ed.* **2010**, *49*, 6352–6356.

[11] a) L. F. Chibotaru, L. Ungur, A. Soncini, *Angew. Chem.* **2008**, *120*, 4194–4197; *Angew. Chem. Int. Ed.* **2008**, *47*, 4126–4129; b) J. Luzon, K. Bernot, I. J. Hewitt, C. E. Anson, A. K. Powell, R. Sessoli, *Phys. Rev. Lett.* **2008**, *100*, 247205; c) L. Ungur, W. V. d. Heuvela, L. F. Chibotaru, *New J. Chem.* **2009**, *33*, 1224–1230.

[12] a) D. I. Plokhov, A. K. Zvezdin, A. I. Popov, *Phys. Rev. B* **2011**, *83*, 184415; b) A. I. Popov, D. I. Plokhov, A. K. Zvezdin, *Europhys. Lett.* **2009**, *87*, 67004; c) A. Soncini, L. F. Chibotaru, *Phys. Rev. B* **2010**, *81*, 132403.

[13] a) B. Hussain, D. Savard, T. J. Burchell, W. Wernsdorfer, M. Murugesu, *Chem. Commun.* **2009**, 1100–1102; b) H. Ke, G.-F. Xu, L. Zhao, J. Tang, X.-Y. Zhang, H.-J. Zhang, *Chem. Eur. J.* **2009**, *15*, 10335–10338; c) H. Tian, Y.-N. Guo, L. Zhao, J. Tang, Z. Liu, *Inorg. Chem.* **2011**, *50*, 8688–8690; d) S.-Y. Lin, Y.-N. Guo, Y. Guo, L. Zhao, P. Zhang, H. Ke, J. Tang, *Chem. Commun.* **2012**, *48*, 6924–6926.

[14] a) S. D. Jiang, B. W. Wang, G. Su, Z. M. Wang, S. Gao, *Angew. Chem.* **2010**, *122*, 7610–7613; *Angew. Chem. Int. Ed.* **2010**, *49*, 7448–7451; b) R. A. Layfield, J. J. W. McDouall, S. A. Sulway, F. Tuna, D. Collison, R. E. P. Winpenny, *Chem. Eur. J.* **2010**, *16*, 4442–4446; c) M. T. Gamer, Y. Lan, P. W. Roesky, A. K. Powell, R. Clérac, *Inorg. Chem.* **2008**, *47*, 6581–6583.

[15] R. Sessoli, A. K. Powell, *Coord. Chem. Rev.* **2009**, *253*, 2328–2341.

[16] S. Carretta, E. Liviotti, N. Magnani, P. Santini, G. Amoretti, *Phys. Rev. Lett.* **2004**, *92*, 207205.

[17] J. Long, F. Habib, P. H. Lin, I. Korobkov, G. Enright, L. Ungur, W. Wernsdorfer, L. F. Chibotaru, M. Murugesu, *J. Am. Chem. Soc.* **2011**, *133*, 5319–5328.

[18] a) Y.-N. Guo, G.-F. Xu, P. Gamez, L. Zhao, S.-Y. Lin, R. P. Deng, J. Tang, H. J. Zhang, *J. Am. Chem. Soc.* **2010**, *132*, 8538–8540; b) Y.-N. Guo, G.-F. Xu, Y. Guo, J. Tang, *Dalton Trans.* **2011**, *40*, 9953–9963.

[19] a) K. C. Mondal, A. Sundt, Y. Lan, G. E. Kostakis, O. Waldmann, L. Ungur, L. F. Chibotaru, C. E. Anson, A. K. Powell, *Angew. Chem.* **2012**, *124*, 7668–7672; *Angew. Chem. Int. Ed.* **2012**, *51*, 7550–7554; b) Y.-N. Guo, G.-F. Xu, W. Wernsdorfer, L. Ungur, Y. Guo, J. Tang, H.-J. Zhang, L. F. Chibotaru, A. K. Powell, *J. Am. Chem. Soc.* **2011**, *133*, 11948–11951.

[20] L. F. Chibotaru, L. Ungur, in Programs SINGLE_ANISO and POLY_ANISO **2006**, University of Leuven.

[21] F. Tuna, C. A. Smith, M. Bodensteiner, L. Ungur, L. F. Chibotaru, E. J. L. McInnes, R. E. P. Winpenny, D. Collison, R. A. Layfield, *Angew. Chem.* **2012**, *124*, 7082–7086; *Angew. Chem. Int. Ed.* **2012**, *51*, 6976–6980.